Water vapor sorption behavior of wildfire-burnt soil

Idil Deniz Akin[1*] and Taiwo O. Akinleye[2]

[1*]Corresponding author, Assistant Professor and Colf Distinguished Professor in Geotechnical Engineering, Washington State University, Department of Civil and Environmental Engineering, Pullman, WA 99164, idil.akin@wsu.edu; 509-335-0568.

[2]Graduate Research Assistant, Washington State University, Department of Civil and Environmental Engineering, Pullman, WA 99164.

Abstract: Wildfires and associated wetting-induced slope stability issues (i.e., erosion, shallow landslides) are common problems all around the world. The water retention mechanism of the burnt soil after a severe wildfire is adsorption followed by capillary condensation as saturation increases. During this time, soil is more susceptible to runoff-dominated erosion and associated debris flows. The water vapor sorption behavior of wildfire-burnt soil and wildfire ash is not fully known. This study investigates the evolution of water vapor sorption behavior of wildfire-burnt soil over a year and the impact of wildfire ash on the sorption behavior of burnt soil. Soil samples were collected from the surface and from 50 cm depth, and ash samples were collected from the surface at varying times after the 2019 Williams Flats Wildfire in Colville Indian Reservation. Soil water retention curves of the surface soil and 50 cm soil were measured using a potentiometer. Hysteretic water vapor sorption isotherms were obtained along adsorption and desorption paths using a dynamic water vapor sorption analyzer. Several different parameters including maximum adsorbed water content, degree of hysteresis, specific surface area, and transition relative humidity were calculated from water vapor sorption isotherms and used to evaluate the sorption behavior of wildfire-burnt soil and wildfire ash. The results indicate that (i) wildfire ash is hydrophilic, has an active surface, and contributes to water retention; and (ii) spatial redistribution of ash may result in fluctuations in the water retention of burnt soil over time.

Introduction

Wildfire occurrence and severity have been increasing globally in both size and frequency in recent decades (e.g., Dennison et al. 2014, Westerling 2016). In the Western United States, the wildfires in summer are typically followed by heavy rainfall or snow events in fall and winter. In addition to the immediate loss of life, property, and habitat due to wildfires, slopes burnt by intense wildfires are more susceptible to surficial stability issues (i.e., runoff dominated erosion and precipitation-induced shallow landslides) during the warm season (e.g., Cannon et al. 2003, Robichaud et al 2013, Staley et al. 2017). Wildfire occurrence and severity is expected to increase with climate change due to projected increases in summer droughts, making more slopes prone to surficial stability issues (e.g., Holz and Veblen 2011).

The changes in hydrologic behaviour of soil are the primary reasons for post-wildfire runoff-dominated erosion and associated debris flows. Water repellent conditions of the burnt soil and the presence of wildfire ash on the surface are considered as the primary factors (e.g., Robichaud et al. 2016, DeBano 2000). Ash is the particulate residue from a wildfire and it consists of mineral materials or inorganics and charred organic compounds (Bodi et al. 2014). The organic fraction consists of the residue from burnt aboveground vegetation, burnt organic soil, and sometimes unburnt organic materials (e.g., Bodi et al. 2014). The inorganic fraction consists of silicates, oxides, phosphates, carbonates, sulphates, and amorphous minerals (e.g., Bodi et al. 2014, Ulery et al. 1993, Vassilev et al. 2010). Wildfire ash from high severity wildfires is typically hydrophilic and forms an expansive layer at the surface. Both the organic and inorganic components of hydrophilic wildfire ash contribute to water retention. Whereas, for lower temperature fires (350 °C), ash is hydrophobic (e.g., Doerr et al. 2000, Ebel et al. 2012, Bodi et al. 2011). Depending on the thickness and properties of the ash, the ash layer may act as a hydraulic

barrier at the surface because of increased water repellency or decreased hydraulic conductivity, resulting in decreased infiltration rates (e.g., Doerr et al. 2000). In addition to affecting the infiltration rate, the presence of wildfire ash was shown to change the saturated hydraulic conductivity, sorptivity, and soil water retention curve (e.g. Ebel 2012, Ebel and Moody 2013), indicating that the stability of hillslopes in unsaturated conditions is affected by the presence of ash and its water retention behavior. The water repellency of the burnt soil is associated with "hyper-dry" conditions, where suction values are greater than 10^4 kPa (e.g., Moody and Ebel 2012). Other factors such as the condensation of water-repellent organic compounds upon combustion also contribute to the formation of a water-repellent soil surface, however this type of water repellency is most profoundly seen at temperatures between 175 °C and 200 °C and not typically observed for temperatures over 270 °C - 300 °C as higher temperatures destroy the organics (e.g., Doerr et al. 2000, DeBano 1981, DeBano et al. 1976). The dominant water uptake mechanism of the "hyper-dry" water repellent soil is adsorption (e.g., Rossi and Nimmo 1994, Silva and Grifoll 2007).

Immediately after the wildfire, the ash typically covers the entire soil surface, whereas over time, only patches of ash are visible on the surface and some percentage may be mixed with soil, transported through wind or runoff and redistributed (e.g., Woods and Balfour 2008, Bodi et al. 2014, Pereira et al. 2013). Therefore, the first wet season after a wildfire is typically the most critical for surficial stability issues. When the water-repellent surface soil that is covered with an expansive hydrophilic ash layer experiences infiltration, the ash retains water and potentially swells, but liquid water cannot infiltrate the hyper-dry soil even under high hydraulic gradients until all the sorption sites of the burnt soil are occupied with water molecules and the water uptake mechanism transitions into capillary condensation (e.g., Moody and Ebel 2012, Akin and Likos

2017). Until the adsorption of burnt soil is completed, the hillslope is more prone to runoff-dominated erosion and associated debris flows. In addition, during this time, the increased runoff may result in excessive floods.

The water vapor adsorption by burnt soil is critical to promote infiltration and prevent potential catastrophic events. However, to our knowledge, there is currently no comprehensive study that investigates the water vapor sorption behaviour of wildfire-burnt soils. Therefore, this study investigates the evolution of water vapor sorption behavior of a wildfire-burnt soil over one year after the fire. The water vapor sorption behavior of wildfire ash and charred biomass samples are also investigated to identify potential impacts of wildfire ash on the sorption behavior of burnt soil. A number of parameters (maximum adsorbed water content, specific surface area, degree of hysteresis, transition relative humidity (*RH*) between adsorption and capillary condensation) were obtained from the water vapor sorption isotherms to provide a quantitative comparison of the sorption behavior over time.

Background

Water vapor sorption isotherms

The soil surface characteristics that control adsorption and interaction between water molecules and material surfaces can be evaluated using water vapor sorption isotherms, which are unique for each soil. The general shape of the isotherm can give information on sorption sequence. Most soils show Type II isotherm shape (Brunauer 1945), which indicates incremental adsorption on mineral surfaces as molecular monolayers until adsorbed films grow to a thickness that they are no longer influenced by the particle surfaces. Adsorbed water content uniformly increases with increased *RH*. For hydrophobic surfaces, adsorbed water content initially increases uniformly with

increasing *RH*, however at higher *RH*, adsorbed water content can show a non-uniform behavior with *RH* (Adamson 1968). Fig. 1 illustrates the characteristic shape of Type II isotherms (solid line) and isotherms of materials with hydrophobic surfaces (dashed line). However, for hydrophobic soils, the isotherm shape that is typical to hydrophobic surfaces is not observed (e.g., Miyamoto et al. 1971). Instead, hydrophobic soils were found to show Type II isotherm shape, but with different amounts of adsorbed water content (e.g., Chen et al. 2018).

In addition to the general shape, several parameters calculated from the water vapor sorption isotherms can be used to identify the surface properties and mineral structure of soils (e.g., Akin and Likos 2014, Lu and Khorshidi 2015), making sorption isotherms a valuable tool for soil characterization.

Study site and sample collection

The Williams Flats Fire started on August 2, 2019 in Colville Indian Reservation, near Keller, WA, USA and burned 17,987 ha of forest land before being contained on August 25, 2019. The burnt vegetation was ponderosa pine (*Pinus ponderosa*) and mixed conifer, in addition to light logging slash and different brush and grass species including antelope bitterbrush (*Purshia tridentata*) and *Ceanothus*. The field soil sampling location was selected in a high burn severity area as defined by Parsons et al. (2010; Fig. 2).

Bulk and intact core soil samples were collected from the surface and from 50 cm depth in October 2, 2019 to run standard soil classification and water repellency tests and determine in-situ void ratio. Samples were collected in a 2 m radius around a burnt tree. Both the surface soil and 50 cm soil were classified as silty sand (SM) according to Unified Soil Classification System, USCS (ASTM D2487). Particle size distribution curves are shown in Fig. 3. Surface soil has 53%

sand, 37% silt, and 10% clay and 50 cm soil has 1% gravel, 68% sand, 25% silt, and 6% clay (Table 1). Fines are classified as non-plastic. The organic content was measured with loss on ignition (LOI) test, wherein soil samples were first dried in 105 °C oven and then kept in a 550 °C furnace for 4 h. The organic content in surface soil and 50 cm soil was found as 9.3% and 2.8%, respectively (Table 1).

Subsequent field visits took place in November 2019, May 2020, June 2020, July 2020, August 2020, and September 2020 to collect bulk soil (from the surface and 50 cm depth) and ash samples. During all field visits, the soil samples were collected 2 m away from the same burnt tree. Ash samples were collected from the surface in all the visits except for November 2019 and September 2020 visits under the same burnt tree. Ash was visible in all the visits except for the November 2019 visit, when the ground surface was frozen and covered with snow. Sample collection could not proceed between November 2019 and May 2020 because the site was not accessible due to heavy snow cover.

Samples were collected from 50 cm depth in addition to surface to evaluate possible vertical redistribution of ash through macropores. The 50 cm soil was not affected by the wildfire heat; therefore, changes in soil properties over time because of a recovery from the wildfire heat is not expected. In addition, the soil samples collected within the 2 m radius is not expected to show a considerable spatial variability. To test the uniformity of the 50 cm soil layer, soil samples were collected in October 2019 from two pits that were ~200 m away from each other. Standard soil classification tests showed identical soil properties indicating the likely uniformity of the soil layer at 50 cm depth within the test area. Therefore, if any change is observed in the 50 cm soil behavior, that would be an indication of the presence of an additional water uptake agent such as the hydrophilic wildfire ash.

Methods

Water droplet penetration time

Water droplet penetration time (WDPT) tests (Van't Woudt 1959) were conducted on October 2019 surface and 50 cm samples and surface samples for May 2020, June 2020, and July 2020. Soil samples were kept in 8 cm diameter, 5 cm height sampling rings during the tests. The WDPT test was conducted with 16 equally-spaced deionized water droplets placed on the soil surface using a standard medicine dropper. The soils were classified as "non-repellent" for WDPT values less than 1 s, "slightly repellent" for WDPT between 1 s and 60 s, and "strongly repellent" for WDPT between 60 s and 600 s (King 1981, Chenu et al. 2000). The tests were terminated if the water droplets are still not absorbed after 20 min. and the soil was then classified as "severely repellent".

Water vapor sorption isotherms

Hysteretic water vapor sorption isotherms of the soil and ash samples were measured at 25°C ± 0.2°C using a vapor sorption analyzer (VSA) operating in dynamic dew point isotherm (DDI) mode (METER Group, Pullman, WA, USA). The bulk field samples were first homogenized in 5 gallon buckets. Approximately 10 g of representative soil was sampled from the buckets, the roots were removed, the samples were dried in a 105 °C oven to replicate hyper-dry conditions, and then passed through #40 sieve. 1.00 ± 0.01 g dry soil sample or 0.600 ± 0.02 g ash sample was placed in a stainless steel VSA cup as a thin uncompacted layer covering the cup surface. The sample cup was then placed into the closed chamber of VSA and continuously wetted (for adsorption) or dried (for desorption) by circulating either a vapor-saturated or desiccated air stream through the chamber. The samples were brought to 3% *RH* followed by an adsorption curve

177 up to 95% *RH*, then by a desorption curve back down to 3% *RH* in 1% *RH* increments. The VSA
178 automatically controls the *RH* in the sample chamber and moves to the next *RH* increment after
179 taking a sample mass measurement that corresponds to the chamber *RH*, which is measured using
180 a chilled-mirror dew point sensor (Leong et al. 2003, Campbell et al. 2007). The sorption isotherms
181 obtained in DDI mode and the traditional equilibrium mode is within 10% - 15% and the
182 reproducibility of DDI mode is 6% (Likos and Lu 2003).

183 ***Specific Surface Area***

184 The specific surface areas (SSAs) were calculated from the desorption isotherms (Eqn. 2)
185 following the Akin and Likos (2014) method, which models water vapor sorption using the BET
186 theory (Eqn. 1, Brunauer et al. 1938).

187 $$\frac{P}{X(P_0 - P)} = \frac{1}{X_m C} + \frac{C-1}{X_m C} \cdot \frac{P}{P_0} \quad (1)$$

188 $$SSA = \frac{X_m}{M_w} NA \quad (2)$$

189 where X is the mass of sorbate per unit mass of sorbent (g/g) at vapor pressure P and temperature
190 T, P_0 is the saturated vapor pressure of the sorbate at the same temperature, X_m is the quantity
191 adsorbed (g/g) when the sorbent is covered with a monolayer, C is the BET constant that shows
192 the heat of hydration, M_w is the molecular mass of water, N is the Avogadro's number, and A is
193 the area covered by one H_2O molecule. For water vapor, the ratio P/P_0 is equal to the relative water
194 vapor pressure or *RH*, and X is gravimetric water content.

195 ***Degree of hysteresis***

196 The degree of hysteresis (D_h) of the samples was quantified from water vapor sorption
197 isotherms according to Lu and Khorshidi (2015) as:

$$\frac{\sum_{i=1}^{N} D_{hi}}{N} = \frac{\sum_{i=1}^{N} \frac{w_{di} - w_{wi}}{w_{mi}}}{N} \quad (3)$$

where w_{di} is the water content at point *i* during desorption, *N* is the total number of points, w_{wi} is the water content at point *i* during adsorption, and w_{mi} is the average water content of the adsorption and desorption states at point *i*.

Soil Water Retention Curve (SWRC)

The soil water retention curve (SWRC) of the October 2019 soil samples (i.e., surface and 50 cm) was measured using a water potential meter incorporating the chilled-mirror dew point technique (WP4C, METER Group, Pullman, WA). Bulk soil was oven-dried (105 °C) and mixed with deionized water. The proportions, by mass, of deionized water and dry soil were controlled to achieve target degree of saturations, *S* (between 0.1 and 0.8, in increments of 0.1) at the field void ratio (1.57 for surface and 0.57 for 50 cm sample) that was determined using intact core samples.

The soil-water mixture was homogenized using a mortar and pestle and compacted into steel WP4C cups at a constant volume. The cups were sealed with plastic caps after compaction and equilibrated for 24 h before suction measurement. Gravimetric water content of the samples was measured after suction measurement and converted to degree of saturation (will be referred as saturation, *S*) using the compaction (or field) void ratio.

Adsorption-Capillary Condensation Transition

When adsorbed water films on material surfaces grow to the thickness that they are no longer influenced by the particle surfaces, the dominant water uptake mechanism transitions into capillary condensation. At this point, the isotherm presents as more rapid water uptake starting at

219 a *RH* about between 80% and 90%. This transition can be quantitatively interpreted following a
220 number of methods (e.g., Philip 1977, Prost et al. 1998, Tuller et al. 1999, Frydman and Baker
221 2009, Leão and Tuller 2014). The Prost et al. (1998) approach uses the Frenkel-Halsey-Hill (FHH)
222 isotherm model (Frenkel 1955, Halsey 1948, Hill 1952) that was developed for multilayer sorption
223 on heterogeneous surfaces. The FHH model is defined as:

224 $$R_H = \frac{1}{\exp\left(\frac{K}{\theta^s}\right)} \quad (4)$$

225 where θ is the fractional coverage (w/X_m), w is the gravimetric water content, K is a parameter that
226 is function of the energy of adsorption of the first layer, and the exponent s depends on the surface
227 structure of the sorbent. An FHH plot is created by plotting $\ln(w)$ versus $\ln[\ln(1/R_H)]$, where non-
228 linearity represents a deviation from multilayer adsorption and therefore indicates monolayer
229 adsorption (at low w) and the start of capillary condensation (at higher w) (e.g., Badmann et al.
230 1981, Pierce 1960, Prost et al. 1998, Akin and Likos 2017).

231 **Results and Discussion**

232 ***Water repellency***

233 Water repellency of the October 2019 surface and 50 cm samples and surface samples for
234 May 2020, June 2020, and July 2020 were evaluated using WDPT test at in-situ water content
235 (Table 2). 50 cm sample adsorbed water droplets in less than 1 s and was classified as "non-
236 repellent". The May 2020 and June 2020 surface samples absorbed the water droplets in less than
237 5 s, in average, with local spots showing "non-repellent" to "slightly repellent" behavior. For the
238 October 2019 surface sample, the average absorption time was 110 s (with a range between 1 s
239 and 300 s), and for the July 2020 sample the average absorption time was 420 s (with a range

between 1 s and 1200 s) and therefore both were classified as "strongly repellent" with local spots ranging from non-repellent to severely repellent behavior.

The water repellency values reported serve as baseline as they are actual water repellency values, which depend on water content (e.g., Dekker et al. 2001). The dependency of water repellency on water content was documented in the literature, where water repellency increased at hyper-dry conditions and decreased at higher water contents with the transition from an adsorption-dominated water uptake mechanism to a capillarity-dominated mechanism (e.g., Doerr and Thomas 2000, Dekker and Ritsema 1996). The soil water repellency in the field is a dynamic property and in addition to the water content, vegetation, bacteria and fungi living in the soil, and soil organic matter also generate water repellent conditions (e.g., Doerr et al. 2000). Depending on these dynamic factors, the surface soil may show different degrees of water repellency at a time after the wildfire, as observed in our results. When the soil shows water repellent behavior in dry conditions, the initial water uptake mechanism is adsorption.

Soil water retention curve

The WP4C data covered a wide range of saturations (up to 0.6 *S*) for both the surface and 50 cm soil (Fig. 4a). The SWRC of the surface soil and the 50 cm soil showed a similar behavior for data points between ~0.3 *S* and 0.6 *S* but differed at lower saturations, where 50 cm soil maintained higher saturations at any suction level. The SWRCs in Fig. 4a represent the retention behavior of the surface soil and 50 cm soil in the field as they were measured at the field void ratio. However, the influence of additional soil water uptake agents (i.e., wildfire ash, fines, and organics) on water retention behavior is not clear because of the void ratio difference. Therefore, the SWRC data was also plotted with gravimetric water content (Fig. 4b) and the VSA data was added to the WP4C data. The water content based SWRC shows that the surface soil retains more

263 water at any suction value. This is primarily attributed to the higher fine and organic content of the
264 surface soil.

265 ***Water vapor sorption behavior***

266 Water vapor sorption isotherms of the surface soil, 50 cm soil, and ash samples collected
267 in October 2019 were plotted along both the adsorption and desorption paths (Fig. 5). The
268 isotherms showed the general characteristics of Type II isotherms (Fig. 1; Brunauer 1945) and did
269 not show characteristics of adsorption by hydrophobic surfaces (Adamson 1968). This was
270 consistent with literature findings for soils, where water repellency did not affect the isotherm
271 shape, heat of adsorption, monolayer coverage or integral free energy of adsorption and therefore
272 models such as BET were found to be valid for such isotherms (Miyamoto et al. 1971). The surface
273 soil showed higher water retention compared to 50 cm soil (Fig. 5) as also observed in the SWRC
274 (Fig. 4). The maximum adsorbed water content at 95% *RH* was 0.024 g/g for 50 cm soil and 0.048
275 g/g for the surface soil. Wildfire ash showed the highest water retention with a maximum adsorbed
276 water content of 0.065 g/g at 95% *RH*. All three isotherms showed a hysteretic behavior (Fig. 5),
277 where more water was retained on particle surfaces during desorption than during adsorption.
278 Based on Eqn. 3, the average degree of hysteresis was calculated as ~0.4 for surface soil, ~0.2 for
279 50 cm soil, and ~0.5 for ash.

280 Hysteresis in water vapor sorption isotherms increases with the presence of high adsorbent
281 particles that change their structure upon wetting. The examples of such particles are expansive
282 clay minerals, polymers, and biofilms (e.g., Lu and Khorshidi 2015, Akin and Likos 2016a, Shariq
283 et al. 2021). Small (~0.1) degree of hysteresis values show that the primary water uptake
284 mechanism is surface hydration, whereas increasing values indicate cation hydration contributes
285 to water uptake in addition to particle surface hydration. While a degree of hysteresis of 0.2 is

common for silty soils, the values above 0.4 are seen in smectite-rich clays, where cation hydration and crystalline swelling are the dominant mechanisms at low *RH* (e.g., Lu and Khorshidi 2015, Akin and Likos 2020). Alternatively, degree of hysteresis values over 0.5 were calculated for highly adsorbent polymers, where water that is entrapped in hydrated polymer structure cannot be readily desorbed as *RH* decreases (e.g., Cohen et al. 1992, Akin and Likos 2016a). The high degree of hysteresis (0.5) of wildfire ash was attributed to changes in ash structure with increasing *RH* to accommodate more water molecules and the high degree of hysteresis of surface soil was attributed to the presence of wildfire ash. Our previous studies on Wyoming bentonite and Georgia kaolinite, which are the end member clays in terms of water retention behavior (Akin and Likos 2014), present a general range of hysteresis expected in clays, between 0.34 (for Wyoming bentonite) and 0.08 (for Georgia kaolinite). The clay content in surface soil is only 10%, yet the surface soil has a degree of hysteresis of 0.4. Even if the clay minerals were sodium-montmorillonite as they are in Wyoming bentonite, the degree of hysteresis would be expected to be less than 0.34. Therefore, the high degree of hysteresis (0.4) of surface soil was attributed to the presence of organics. In October 2019, when the vegetative and microbial recovery isn't complete, the main source for organics is attributed to be wildfire ash.

Specific surface areas (SSAs) were quantified using Eqn. 2 to evaluate the structure of the soil and ash samples and to understand the interactions between water molecules and soil or ash surfaces. The SSA was calculated as 54 m^2/g for surface soil, 24 m^2/g for 50 cm soil, and 76 m^2/g for ash. 15-60 m^2/g is common for silty soils, whereas values above that are more commonly seen in clayey soils with more active surfaces (e.g., Akin and Likos 2016b). The high SSA of wildfire ash indicates that wildfire ash has an active surface and contributes to water retention.

Water vapor sorption isotherms (Fig. 5) show indirect evidence for the transition between adsorption and capillary condensation as quantified by the FHH model (Eqn. 6). Fig. 6 is the FHH plot of the surface soil and shows the transitions at *RH* values 31% and 69%, interpreted to reflect the transitions between monolayer adsorption and multilayer adsorption (31% *RH,* 0.012 g/g *w*) and multilayer adsorption and capillary condensation (69% *RH,* 0.024 g/g *w*). Based on the FHH analysis, the adsorption-capillary transition was found to be at 54% *RH (*0.009 g/g *w)* for the 50 cm soil and at 75% *RH (*0.035 g/g *w)* for wildfire ash. The results indicate that surface soil will be more prone to runoff-dominated erosion and associated debris flows until it is hydrated to 0.024 g/g water content.

Evolution in water vapor sorption behavior over time

The isotherms of 50 cm soil samples all showed hysteretic behavior and only the adsorption curves are plotted for clarity (Fig. 7a). A variation in water vapor sorption isotherms is observed over time. The maximum adsorbed water content was within ~30%, varied between 0.024 g/g (for October 2019) and 0.032 g/g (for May 2020).

The sorption isotherms of the surface soil stayed in a relatively narrow range (i.e., maximum adsorbed water content was within ~20%) except for the November 2019 sample (Fig. 7b). The sorption isotherms of the surface samples collected in October 2019, June 2020, July 2020, and September 2020 showed a relatively similar behavior with a maximum adsorbed water content of 0.048 g/g for June 2020 and October 2019, 0.044 g/g for July 2020, and 0.043 g/g for September 2020. May 2020 and August 2020 samples displayed a slightly lower sorption behavior with a maximum adsorbed water content of 0.040 g/g. The November 2019 surface soil showed the lowest water retention with a maximum adsorbed water content of 0.026 g/g, almost half of the June 2020 or October 2019 samples. The low sorption behavior of the November 2019 sample

was attributed to the challenges related to sample collection in snowy winter months. The ground surface was frozen and covered with snow in November. The snow cover was carefully removed for sample collection; however, this process might have also removed ash from the surface. The resulting soil displayed a sorption behavior similar to the 50 cm soil collected in the summer and fall months (Fig. 7a), which showed a maximum adsorbed water content of 0.024 g/g, half of what was observed in June 2020 and October 2019.

The change in sorption behavior of 50 cm and surface samples could be partly because of spatial variability of the soil (expected to be minimum within a 2 m radius area) or repeatability of the measurement (within 6%, Likos and Lu 2003). The comparison of November 2019 surface sample with the rest of the surface samples, the uniformity of the 50 cm layer, and 20%-30% variation in maximum adsorbed water content over time indicate there may be other factors that are responsible from the changes.

The fluctuations in water vapor sorption behavior of the surface and 50 cm soil over time was partially attributed to the redistribution of wildfire ash and its characteristics. In the field, ash can easily be transported and redistributed (both horizontally and vertically) by wind, runoff, soil pores, freeze-thaw cycles, or earthworms (e.g., Topoliantz et al. 2006, Pereira et al. 2013). In addition, other potential factors that change dynamically in a forest environment recovering from a fire and that are challenging to control or measure (regrowth, root decay, microbial life) could be responsible for the changes in sorption behavior over time. Two additional ash samples were collected to evaluate the changes in ash properties over time; one in June 2020 (black) and one in July 2020 (white) from the soil surface ~2 m away from the burnt tree. The ash samples were collected from the same 2 m radius circle at different times after the wildfire, showing the redistribution of ash in the field over time. In addition, two charred biomass samples were collected

354 from the soil surface, under the burned tree bark in May 2020 and August 2020. The isotherms
355 showed different shapes (Fig. 8); the charred biomass samples showed a concave downwards
356 isotherm shape indicating that attraction forces between water and ash surface are only effective
357 closer to the particle surfaces (Halsey 1948). This results in a higher SSA of 188 m^2/g and 158
358 m^2/g for the charred biomass samples collected in May and August respectively, and indicates that
359 at a high *RH*, the water uptake mechanism may not be surface adsorption anymore. For
360 comparison, the SSA of ash samples were 45 m^2/g for white ash (July 2020) and 61 m^2/g for black
361 ash (June 2020). The charred biomass samples were also more adsorbent than the ash samples with
362 maximum adsorbed water contents of 0.128 g/g (May 2020) and 0.115 g/g (August 2020),
363 compared to ash samples with maximum adsorbed water contents of 0.065 g/g (June 2020) and
364 0.080 g/g (July 2020). The white ash collected in July 2020 showed a higher maximum adsorbed
365 water content than both of the black ash samples collected in October 2019 and June 2020. The
366 color of ash is related to combustion completeness, where white ash forms after a more complete
367 combustion between 500 °C and 1400 °C and black ash is formed at lower temperatures (e.g.,
368 Goforth et al. 2005). The constituents of ash change with combustion; therefore, the higher
369 maximum adsorbed water content of white ash is a reflection of the difference in chemical
370 composition. At temperatures up to 500 °C silica and carbonates are the dominant compounds,
371 whereas at higher temperatures carbonates dissociate to oxides (e.g., Ulery et al. 1993, Goforth et
372 al 2005).

373 The evolution in SSA and degree of hysteresis over a year after the wildfire are shown in
374 Fig. 9. Surface soil showed consistently higher SSA (around 55 m^2/g) than 50 cm soil (around 40
375 m^2/g) except for the November sample, where the surface soil showed the same SSA as the 50 cm
376 soil (Fig. 8a). Degree of hysteresis of the surface soil was also generally greater than that of 50 cm

soil, except for November 2019 and July 2020 (Fig. 9b). The low sorption behavior of the November surface sample (Fig. 7b), potentially due to the removal of the ash layer with snow cover, is also reflected in SSA and degree of hysteresis. The trends in SSA and degree of hysteresis are generally in agreement with each other, where an increase in SSA coincides with an increase in the degree of hysteresis.

Field Observations and Interpretations

50 cm soil

There were multiple macropores next to the sampling location that could act as pathways for wildfire ash to migrate into soil. The maximum increase in the retention behavior was seen in May (Fig. 7a), after the snowmelt in March-April and the higher sorption behavior was maintained until the end of September. This indicates that ash could be transported with snowmelt through the macropores. The decay of roots over time could also contribute to an increase in organic matter content, which would increase water retention.

Surface soil

Forests are dynamic systems, especially during the recovery after a wildfire. Additional organic matter due to regrowth and death of seasonal wildflowers and grass, microbial recovery after the fire, and organic matter mixed with soil due to decay of burned roots could change the sorption behavior over time. Summer wildflowers were in full bloom in June and seasonal grass covered the soil surface in May. Both the grass and wildflowers were alive until the end of August and after that they contributed to the soil organic matter content. Our study did not control the organic matter due to regrowth/death, root decay, or microbial recovery. Microbial recovery generally takes a couple months (e.g., Klopatek et al. 1994) and the decay of burned roots starts

days or weeks after the wildfire and can continue for months or even years (e.g., Meyer et al. 2001, May and Gresswell 2003, De Graff 2018). Because of these additional factors that may contribute to the sorption behavior of burnt soils, a definite conclusion cannot be reached to explain the fluctuations in sorption behavior over the year. However, our observations during the field visits showed that unlike the common assumption that ash is transported from the surface through wind and runoff within a couple months (Cerdà and Doerr 2008, Pereira et al. 2013), the ash stayed on the surface up to a year after the fire. In addition, the charred biomass also stayed on the site, and progressively fell on the soil surface from burned tree bark. The water vapor sorption isotherms showed that the properties of ash and charred biomass that were found on the site at varying times after the fire were dynamic over the year. However, they all demonstrated characteristics of a highly surface-active material, as indicated particularly in SSA and degree of hysteresis results. The water vapor sorption behavior of surface samples collected over the year showed that the degree of hysteresis and SSA of surface samples were greater than what would be expected for a silty sand. Therefore, the sorption behavior of ash and surface samples together with field observations indicate that ash is present, has an active surface, and therefore may contribute to the water retention behavior of wildfire-burnt soil over a year after a wildfire.

Practical Implications

This study showed that the dominant water retention mechanism of the surface soil from the study area is adsorption up to 69% *RH (*or 0.024 g/g *w*). This indicates that the burnt hillslopes are more susceptible to runoff-dominated erosion and associated debris flows until the hyper-dry surface soil reaches an equilibrium at minimum 0.024 g/g water content for this particular soil. The debris-flow models could be improved to incorporate the adsorption-capillarity transition water content.

The results of this study also provide the first evidence that (i) wildfire ash has an active surface that contributes to water retention, and (ii) water retention behavior of ash fluctuates over time. This suggests that the hydrologic and therefore mechanical behavior of wildfire-burnt hillslopes may dynamically change over time depending on the ash content and characteristics. Therefore, models that evaluate the stability of burnt hillslopes can be improved to incorporate the fluctuations in ash water retention behavior over time.

Summary, Conclusions, and Future Directions

The hydrologic behavior of surface soil burnt by the 2019 Williams Flats Fire, WA, USA was evaluated over time through the soil water retention curve (SWRC) and water vapor sorption isotherms. Water repellency was measured in surface samples, fluctuating between "non-repellent" and "strongly repellent" over the year. SWRCs of the surface soil and soil collected at 50 cm depth were measured with a potentiometer. More profound differences in SWRCs were observed in lower saturations ($S < 0.4$) or higher suctions. Higher suctions were maintained by the surface soil at any water content. Hysteretic water vapor sorption isotherms of surface soil and ash collected after the fire was contained (in October 2019) were measured using a dynamic vapor sorption approach. The SSA, degree of hysteresis, maximum adsorbed water content, and transition *RH* were calculated from the sorption isotherms. The four different parameters calculated from the samples collected in October 2019 indicated that ash is hydrophilic and has an active surface: The maximum adsorbed water content by ash (0.065 g/g), SSA (76 m^2/g), and average degree of hysteresis (0.5), and transition *RH* between adsorption and capillary condensation (75% *RH*) were representative to a hydrophilic surface active material, such as clay minerals.

The evolution in water vapor sorption behavior over one year was investigated to understand the influence of ash redistribution on the retention behavior of the soil in the field. Adsorption by 50 cm soil increased after the snowmelt in May, and the increased level was maintained during the summer months indicating that vertical movement of ash is possible. Surface samples did not show a particular trend over time and this is attributed to dynamic changes in the forest environment during recovery (i.e., microbial recovery, growth/death of seasonal wildflowers and grass, and root decay). Different ash (black and white) and charred biomass samples found in the field over one year displayed spatial redistribution of ash. Overall, the sorption behavior of soil and ash over one year expanded our understanding of post-wildfire forest environments by showing (i) ash is present on the surface for at least a year after the fire (as observed in the field) and has an active surface that can contribute to water retention through adsorption and (ii) ash is mobile and redistribution (both vertically and spatially) of ash may result in a change in water retention behavior of wildfire-burnt hillslopes.

The results of this study led to initial interpretations and conclusions on the water vapor sorption behavior of wildfire-burnt soil and wildfire ash over time. Future studies could simulate fire in laboratory conditions or use prescribed fires to repeat the tests in a more controlled environment. Measurement of the parameters pre-fire could help in reaching more definite conclusions.

Data Availability Statement

Some or all data, models, or code that supports the findings of this study are available from the corresponding author upon reasonable request.

Acknowledgements

This material is based upon work supported by the National Science Foundation (NSF) under Grant CMMI 1932129. Any opinions, findings, and conclusions or recommendations expressed in this material are those of the authors and do not necessarily reflect the views of NSF. We would like to thank Colville Indian Reservation for providing access to the site and Dr. Peter R. Robichaud and Robert E. Brown for their helps with site selection and field work.

References

Adamson, A.W. 1968. "An adsorption model for contact angle and spreading." *J. Colloid Interface Sci*. 27:180-187.

Akin, I.D., and W.J. Likos. 2014. "Specific surface area of clay using water vapor and EGME sorption methods." *Geotechnical Testing Journal*, 37(6): 1-12, doi: 10.1520/GTJ20140064.

Akin, I.D., and W.J. Likos. 2016a. "Water vapor sorption of polymer-modified bentonites." *Geo-Chicago 2016 Technical Papers*.

Akin, I.D., and W.J. Likos. 2016b. "Evaluation of isotherm models for water vapor sorption behavior of expansive clays." *J. Perf. Const. Fac.,* doi: 10.1061/(ASCE)CF.1943-5509.0000899.

Akin, I.D., and W.J. Likos. 2017. "Implications of surface hydration and capillary condensation to strength and stiffness of compacted clay." *J. Eng. Mech.*, doi: 10.1061/(ASCE)EM.1943-7889.0001265.

Akin, I.D., and W.J. Likos. 2020. "Relationship between water vapor sorption kinetics and clay surface properties." *J. Geotech. Geoenviron. Eng.,* 146(9): 06020015.

ASTM D2487-11, 2017. “Standard Practice for Classification of Soils for Engineering Purposes (Unified Soil Classification System).”Annual Book of ASTM Standards, ASTM International, West Conshohocken, PA.

Badmann, R., N. Stockhausen and M.J. Setzer. 1981, “The statistical thickness and the chemical potential of adsorbed water films,” *Journal of Colloid and Interface Science*, 82(2): 534-542.

Bodi, M.B., J. Mataix-Solera, S.H. Doerr, and A. Cerda. 2011. “The wettability of ash from burned vegetation and its relationship to Mediterranean plant species type, burn severity and total organic carbon content.” *Geoderma,* 160: 599-607.

Bodi, M.B., D.A. Martin, V.N. Balfour, C. Santin, S.H. Doerr, A. Cerda, and J. Mataix-Solera. 2014. “Wildland fire ash: Production, composition and eco-hydro-geomorphic effects.” *Earth-Science Reviews*, 130: 103-127.

Brunauer, S., 1945, “The adsorption of gases and vapors,” *Physical Adsorption*, Vol. 1, Princeton Univ. Press, Princeton.

Brunauer, S., P.H. Emmett, and E. Teller. 1938, “Adsorption of gases in multimolecular layers.” *Journal of American Chemical Society*, Vol. 60, pp. 309-319.

Campbell, G.S., D.M. Smith, and B.L. Teare, 2007. “Application of a dew point method to obtain the soil water characteristic.” *Experimental Unsaturated Soil Mechanics*, T. Schanz (Ed.), Springer, pp. 71-77.

Cannon, S.H., J.E. Gartner, C. Parrett, and M. Parise, 2003. “Wildfire-related debris flow generation through episodic progressive sediment bulking processes, Western USA,” In: Rickenmann, D., Chen, C.L. (eds) Proceedings of 3rd international conference, “Debris-flow

hazards mitigation—mechanics, prediction, and assessment," Davos, Switzerland, pp. 71–82.

Cerdà, A., and S.H. Doerr. 2008. "The effect of ash and needle cover on surface runoff and erosion in the immediate post-fire period." Catena 74, 256–263.

Chen, J., C. Shang, M.J. Eick, and R.D. Stewart. 2018. "Water repellency decreases vapor sorption of clay minerals." *Water Resources Research*, 54(9), 6114-6125.

Chenu, C., Y. Le Bissonnais, and D. Arrouays. 2000. "Organic matter influence on clay wettability and soil aggregate stability." *Soil Sci. Soc. Am.* J. 64:1479-1486.

Cohen, Y., O. Ramon, I.J. Kopelman, and S. Mizrahi. 1992. "Characterization of inhomogeneous polyacrylamide hydrogels" *Journal of Polymer Science: Part B: Polymer Physics,* Vol. 30: 1055-1067.

DeBano, L.F., S.M. Savage, and D.A. Hamilton. 1976. "The transfer of heat and hydrophobic substances during burning." *Soil Sci. Soc. Am. J.* 40, 779-782.

DeBano, L.F., 1981. "Water repellent soils: a state-of-the-art. USDA For. Serv. Gen. Tech. Rep. PSW-46. pp. 21.

DeBano, L.F., 2000. "The role of fire and soil heating on water repellency in wildland environments: a review." *Journal of Hydrology,* 231–232, 195– 206.

De Graff, J.V. 2018. "A rationale for effective post-fire debris flow mitigation within forested terrain." *Geoenvironmental Disasters*, doi: 10.1186/s40677-018-0099-z.

Dekker, L.W., S.H. Doerr, K. Oostindie, A.K. Ziogas, and C.J. Ritsema. 2001. "Water repellency and critical soil water content in a dune sand." *Soil Sci. Soc. Am. J.* 65:1667-1674.

529 Dekker, L.W. and C.J. Ritsema. 1996. “Variation in water content and wetting patterns in Dutch
530 water repellent peaty clay and clayey peat soils.” *Catena* 28: 89–105.

531 Dennison, P.E., S.C. Brewer, J.D. Arnold and M.A. Moritz. 2014. “Large wildfire trends in the
532 western United States, 1984-2011.” *Geophysical Research Letters*, 41: 2928 - 2933.

533 Doerr, S.H., R.A. Shakesby, and R.P.D. Walsh, 2000. “Soil water repellency–its causes,
534 characteristics and hydrogeomorphological significance.” *Earth Sci. Rev*., 51:33–65.

535 Doerr, S.H., and A.D. Thomas. 2000. “The role of soil moisture in controlling water repellency:
536 new evidence from forest soils in Portugal.” *J. Hydrol.* 231/232:134–147.

537 Ebel, B.A., 2012. “Wildfire impacts on soil–water retention in the Colorado Front Range, USA.”
538 Water Resour. Res. 48, W12515. http://dx.doi.org/10.1029/2012WR012362.

539 Ebel, B.A., J.A. Moody, and D.A. Martin. 2012. “Hydrologic conditions controlling runoff
540 generation immediately after wildfire.” *Water Resour. Res.,* 48, W03529,
541 doi:10.1029/2011WR011470.

542 Ebel, B.A. and J.A. Moody, 2013. “Rethinking infiltration in wildfire-affected soils,” *Hydrol.*
543 *Proc*., 1510-1514.

544 Frenkel, J., 1955. *Kinetic Theory of Liquids*, Dover Publications Inc., New York.

545 Frydman, S., and R. Baker. 2009, “Theoretical soil-water characteristic curves based on
546 adsorption, cavitation, and a double porosity model.” *Int. J. Geomech*., 9(6): 250-257.

547 Goforth, B.R., R.C. Graham, K.R. Hubbert, C.W. Zanner. and R.A. Minnich. 2005. “Spatial
548 distribution and properties of ash and thermally altered soils after high-severity forest fire,
549 southern California.” *Int. J. Wildland Fire* 14, 343–354.

550 Halsey, G., 1948, “Physical adsorption on non-uniform surfaces.” *The Journal of Chemical*
551 *Physics*, 16(10): 931-937.
552 Hill, T.L., 1952, “Theory of Physical Adsorption.” *Advances in Catalysis*, Vol. 4, pp. 211-258.
553 Holz, A. and T. Veblen. 2011. "Variability in the Southern Annular Mode determines wildfire
554 activity in Patagonia." *Geophysical Research Letters* 38(14).
555 King, P.M., 1981. “Comparison of methods for measuring severity of water repellence of sandy
556 soils and assessment of some factors that affect its measurement.” *Australian Journal of Soil*
557 *Research* 19: 275–285.
558 Klopatek, C.C., C.F. Freise, M.F. Allen, and J.M. Klopatek. 1994. “Comparisons of laboratory and
559 field burning experiments on mycorrhizae distribution, density and diversity”. *J. Soc. Am.*
560 For. (Twelfth Conference on Fire and Forest Mineralogy, Special. Issue) 94, 762-776.
561 Leão, T.P., and M. Tuller. 2014. “Relating soil specific surface area, water film thickness, and
562 water vapor adsorption.” *Water Resour. Res.*, 50: 7873-7885.
563 Leong, E.C., S. Tripathy, and H. Rahardjo. 2003. “Total suction measurement of unsaturated soils
564 with a device using the chilled-mirror dew-point technique.” *Géotechnique*, 53(2): 173-
565 182.
566 Likos, W.J. and N. Lu. 2003. “Automated humidity system for measuring total suction
567 characteristics of clay.” *Geotech. Test. J.,* Vol. 26, No. 2, pp. 178–189.
568 Lu, N., and M. Khorshidi. 2015, “Mechanisms for soil-water retention and hysteresis at high
569 suction range” *J. Geotechnical and Geoenvironmental Engineering*, 141(8): 04015032.
570 Lu, N., and W.J. Likos. 2004, *Unsaturated Soils Mechanics*, Wiley, New York.

May, C.L., and R.E. Gresswell, 2003. “Processes and rates of sediment and wood accumulation in headwater streams of the Oregon Coast Range, USA.” *Earth Surf. Proc. Landf.,* 28:409–424.

Meyer, G.A., J.L. Pierce., S.H. Wood, and A.J.T. Jull. 2001. “Fire, storms, and erosional events in the Idaho batholith.” *Hydrol Process*, 15:3025–3038.

Miyamoto, S., J. Letey, and J. Osborn. 1972. “Water vapor adsorption by water-repellent soils at equilibrium.” *Soil Science*, 113(3): 180-184.

Moody, J.A., and B.A. Ebel. 2012. “Hyper-dry conditions provide new insights into the cause of extreme floods after wildfire.” *Catena*, 93: 58-63.

Parsons A, P. Robichaud, S. Lewis, C. Napper, and J. Clark. 2010. “Field guide for mapping post-fire soil burn severity.” USDA For. Serv. Gen. Tech. Rep. RMRS-GTR-243.

Pereira, P., A. Cerdà, X. Úbeda, J. Mataix-Solera, V. Arcenegui, and L.M. Zavala. 2013. “Modelling the impacts of wildfire on ash thickness in a short-term period.”. *Land Degrad. Dev*. http://dx.doi.org/10.1002/ldr.2195.

Philip, J.R. 1977. “Unitary approach to capillary condensation and adsorption.” *J. Chem. Phys*. 66(11): 5069-5075.

Pierce, C. 1960. “The Frenkel-Halsey-Hill adsorption isotherm and capillary condensation.” *The Journal of Physical Chemistry*, 64(9): 1184-1187.

Prost, R., A. Benchara and E. Huard. 1998. “State and location of water adsorbed on clay minerals: consequences of the hydration and swelling-shrinkage phenomena.” *Clays and Clay Minerals*, 46(2): 117-131.

592 Robichaud, P.R., S.A. Lewis, L.E. Wagenbrenner, L.E. Ashmun, and R.E. Brown. 2013. "Post-
593 fire mulching for runoff and erosion mitigation part I: Effectiveness at reducing hillslope
594 erosion rates." *Catena*, 105: 75-92.

595 Robichaud, P.R., J.W. Wagenbrenner, F.B. Pierson, K.E. Spaeth, L.E. Ashmun, and C.A. Moffet.
596 2016. "Infiltration and interrill erosion rates after a wildfire in western Montana, USA,"
597 *Catena*, 142: 77-88.

598 Rossi, C., and J.R. Nimmo, 1994. "Modeling of soil water retention from saturation to oven
599 dryness." *Water Resources Research* 30, 701–708.

600 Shariq, A.F., H. Beyenal, and I.D. Akin. 2021. "Biofilm addition improves sand strength over a
601 wide range of saturations." *Biofilm*, doi: https://doi.org/10.1016/j.bioflm.2021.100050.

602 Silva, O., and J. Grifoll. 2007. "A soil-water retention function that includes the hyper-dry region
603 through the BET adsorption isotherm." *Water Resources Research* 43. doi:10.1029/
604 2006WR005325.

605 Staley, D.M., J.A. Negri, J.W. Kean, J.M. Laber, A.C. Tillery, and A.M. Youberg. 2017.
606 "Prediction of spatially explicit rainfall intensity-duration thresholds for post-fire debris flow
607 generation in the western United States." *Geomorphology* 278: 149-162.

608 Topoliantz, S., J.F. Ponge, and P. Lavelle. 2006. "Humus components and biogenic structures
609 under tropical slash-and-burn". *Eur. J. Soil Sci*. 57, 269–278.

610 Tuller, M., D. Or, and L.M. Dudley. 1999. "Adsorption and capillary condensation in porous
611 media: Liquid retention and interfacial configurations in angular pores." *Water Resources*
612 *Research*, 35(7): 1949-1964.

Ulery, A.L., R.C. Graham, and C. Amrhein. 1993. “Wood-ash composition and soil pH following intense burning.” *Soil Sci*. 156, 358–364.

Van’t Woudt, B.D. 1959. “Particle coatings affecting the wettability of soils.” *Journal of Geophysical Research* 64, 263–267.

Vassilev, S.V., D. Baxter, L.K. Andersen, and C.G. Vassileva. 2010. “An overview of the chemical composition of biomass.” *Fuel 89* (5), 913–933.

Westerling, A.L. 2016. “Increasing western US forest wildfire activity: sensitivity to changes in the timing of spring,” *Philosophical Transactions of the Royal Society B*, 371: 20150178.

Woods, S.W., and V.N. Balfour. 2008. “The effect of ash on runoff and erosion after a severe forest fire.” Montana, USA. *Int. J. Wildl. Fire*, 17:535–548.

Table 1: Properties of surface and 50 cm soil collected in October 2019.

	Soil	
	October 2019 surface	October 2019 50 cm
%gravel	-	1
%sand	53	68
%silt	37	25
%clay	10	6
USCS classification	SM	SM
Organic content (%)	9.3	2.8

Table 2: WDPT and water repellency of soils over time.

Soil	Average WDPT (s)	Average water repellency
October 2019 surface	110	strongly repellent
October 2019 50 cm	<1	non-repellent
May 2020 surface	1	slightly repellent
June 2020 surface	4	slightly repellent
July 2020 surface	420	strongly repellent

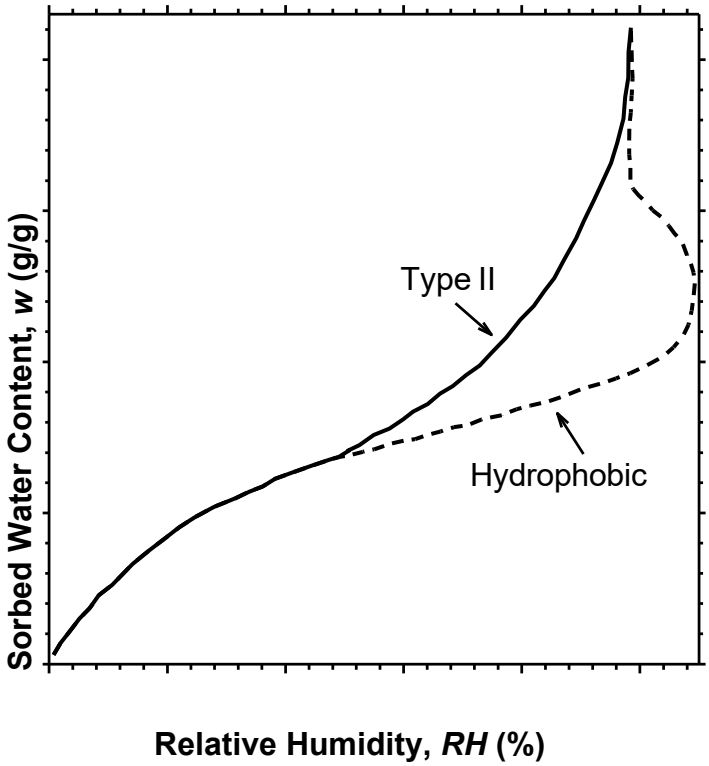

Fig. 1: General shape of a Type II isotherm (solid line) and isotherm of materials with hydrophobic surfaces (after Brunauer 1945 and Adamson 1968).

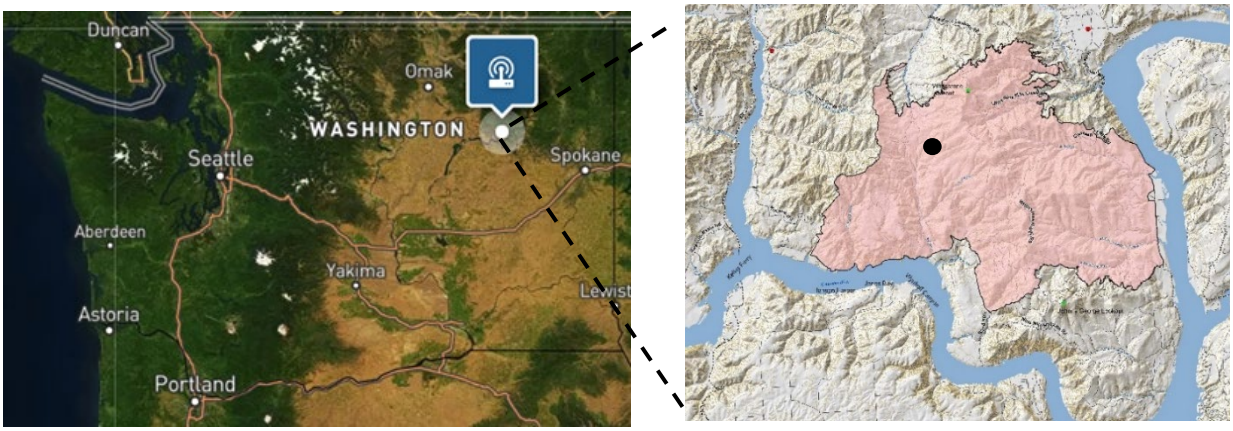

Fig. 2: Location of the site. Sampling location is shown on the burned area map (public information map, inciweb.nwcg.gov) with the black circle.

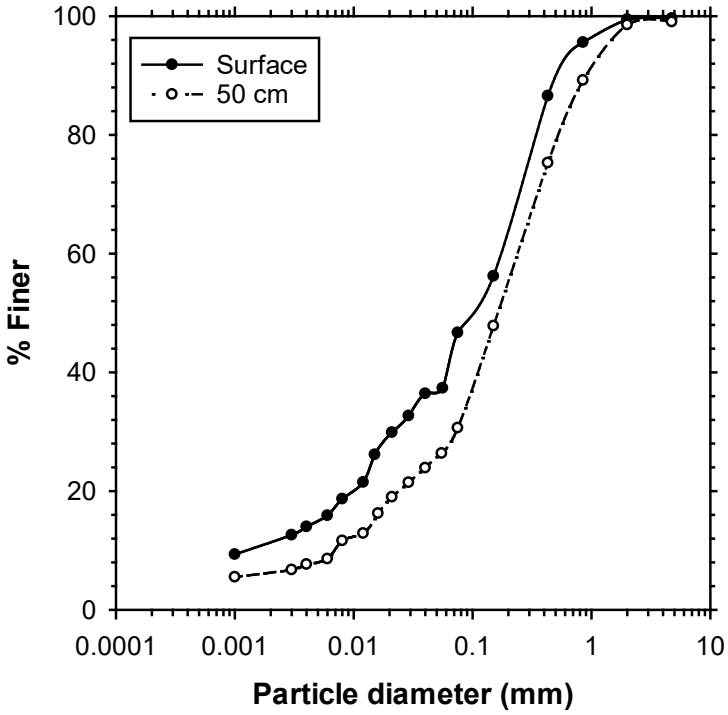

Fig. 3: Particle size distribution curves of surface soil and 50 cm soil. Surface soil % sand = 53, % clay = 10, % silt = 37 ; 50 cm soil % gravel = 1, % sand = 68, % clay = 6, % silt = 25.

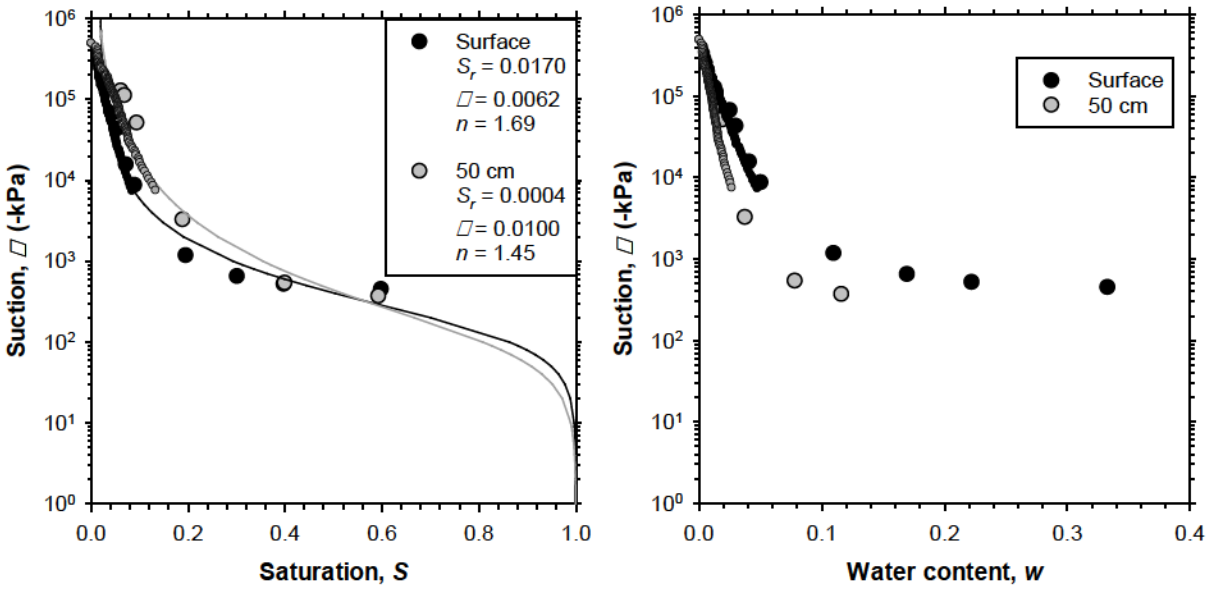

705

706 **Fig. 4:** SWRC of surface soil and 50 cm soil collected in October 2019 with respect to (a)
707 saturation and (b) water content.

708

709

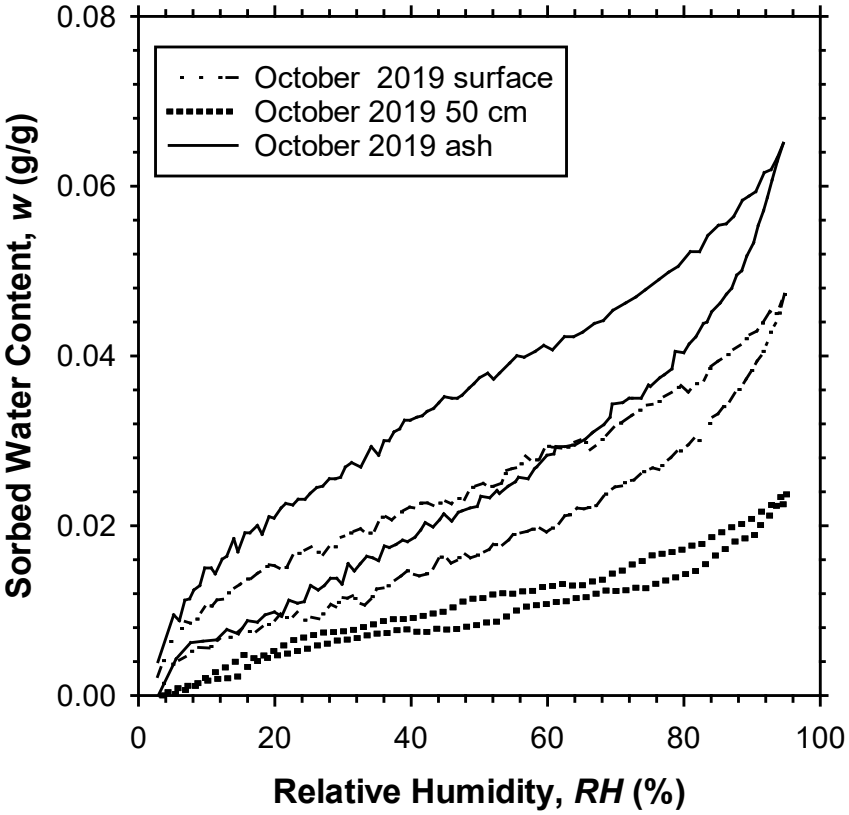

710

711 **Fig. 5.** Water vapor sorption isotherms of surface soil, 50 cm soil, and wildfire ash collected in
712 October 2019.

713

714

715

716

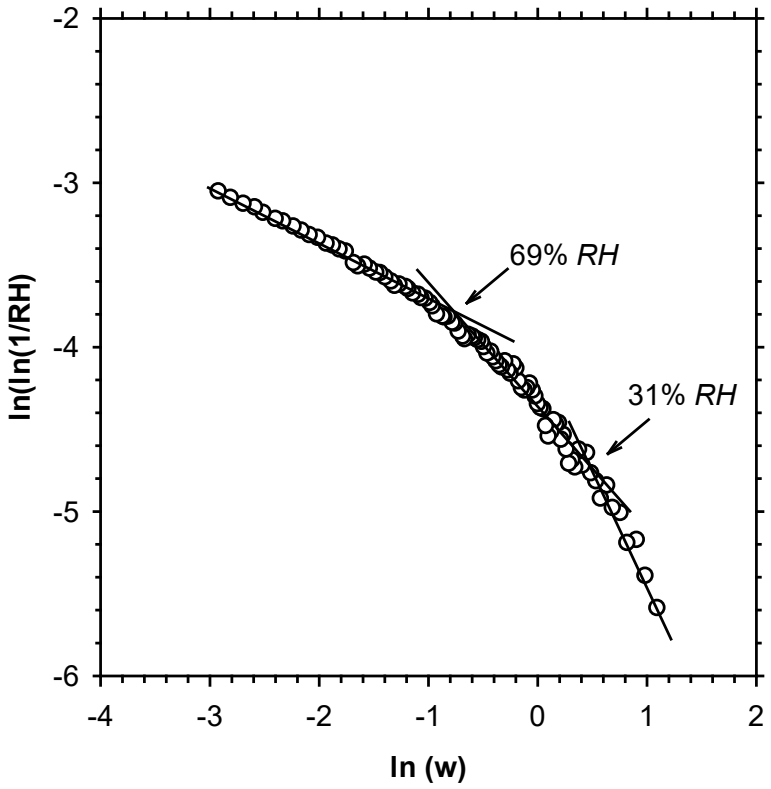

717

718 **Fig. 6:** FHH plot of surface soil. Lines represent different water uptake regimes; capillary
719 condensation, multilayer adsorption, monolayer adsorption (from left to right).

720

721

722

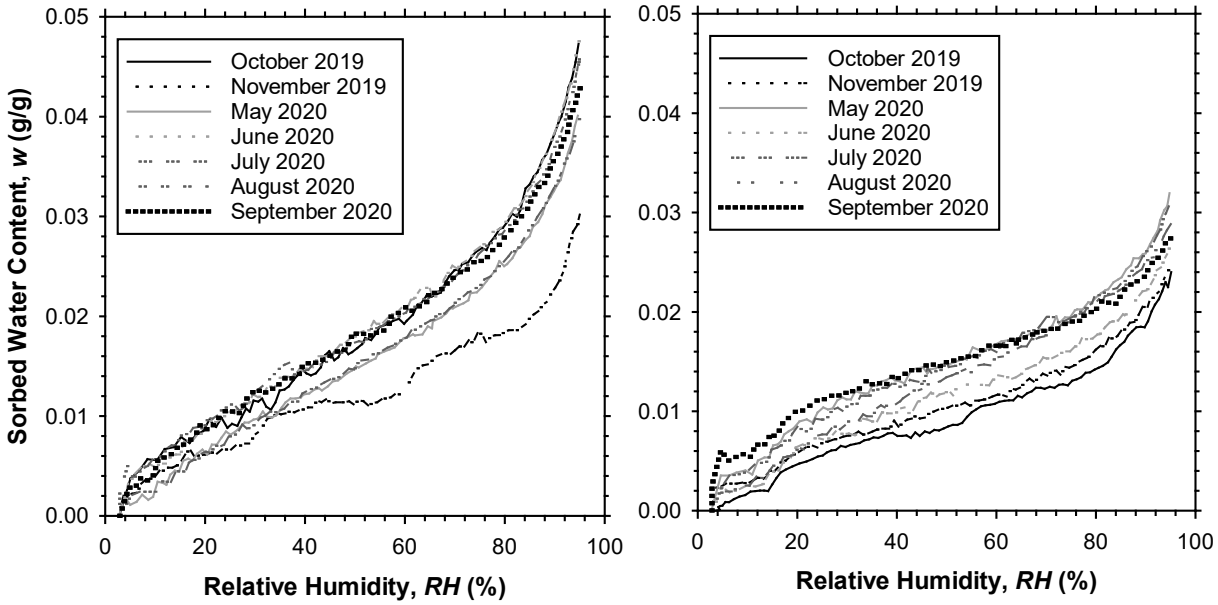

723

724 **Fig. 7:** Water vapor sorption isotherms of (a) 50 cm soil, (b) surface soil over time.

725

726

727

728

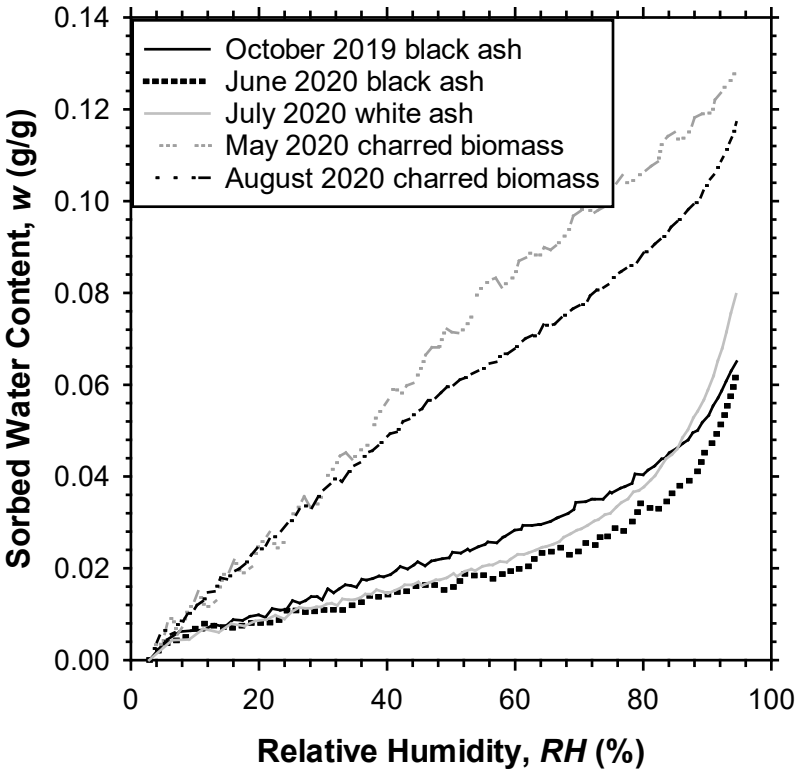

729

730 **Fig. 8:** Water vapor sorption isotherms of different wildfire ash samples collected within 2 m of
731 the same burnt tree.

732

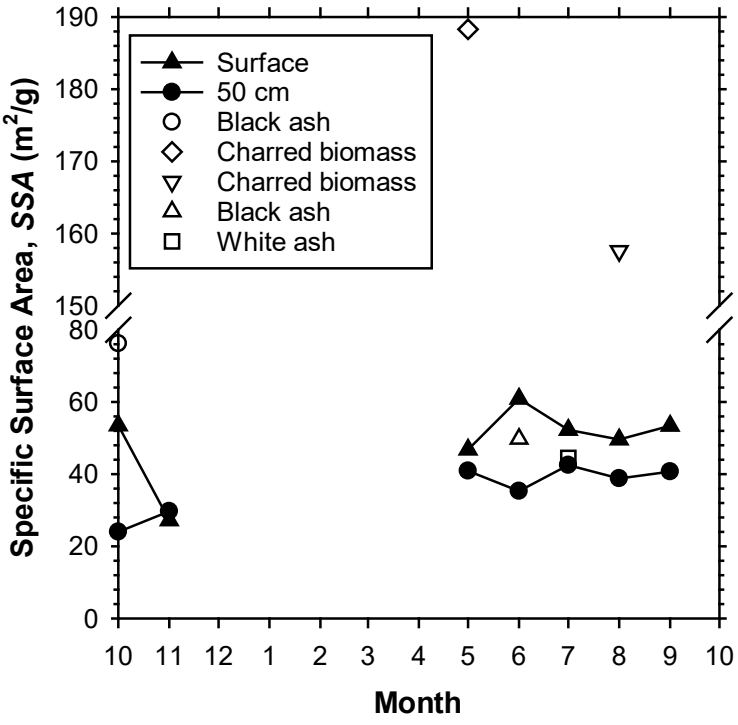

733

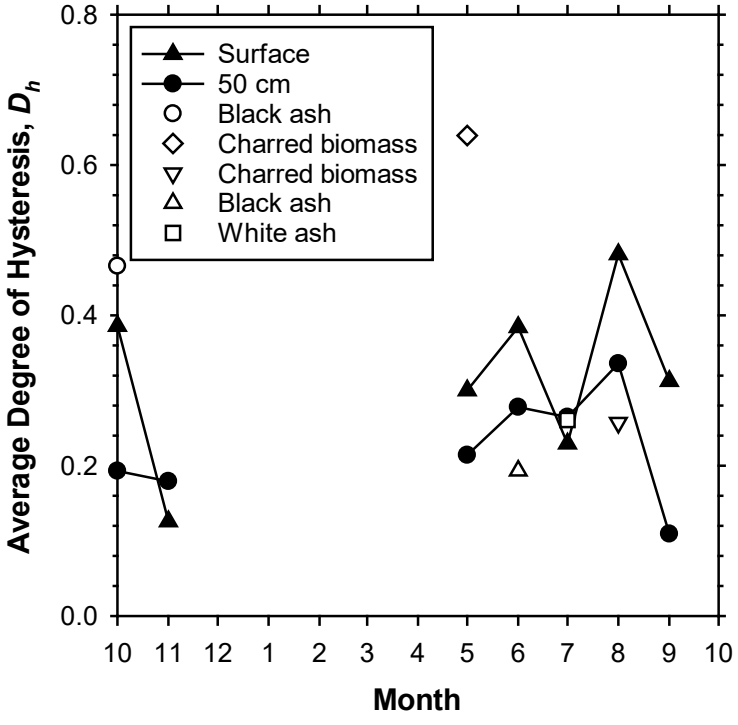

734

735 **Fig. 9:** Evolution in (a) specific surface area, and (b) average degree of hysteresis over one year.
736 Sample collection could not proceed between November 2019 and May 2020 because the site
737 was not accessible due to heavy snow cover.